

Photonics-Based Instantaneous Multi-Parameter Measurement of a Linear Frequency Modulation Microwave Signal

Bowen Zhang, Xiangchuan Wang , and Shilong Pan , *Senior Member, IEEE*

Abstract—A novel approach for simultaneous and instantaneous measurement of the center frequency (CF), bandwidth (BW), pulse width (PW), pulse amplitude (PA), and time of arrival (TOA) of a linear frequency modulation (LFM) pulse signal is proposed and experimentally demonstrated. The approach is based on a linear amplitude comparison function (ACF) obtained by intensity modulation and first-order differentiated phase modulation, which are realized using a polarization modulator, two polarizers, and an optical linear filter. The linearity characteristic of the ACF ensures the ability of the proposed system to measure multiple parameters of an LFM pulse signal. In a proof-of-concept experiment, the measurement errors for CF, BW, PW, PA, and TOA of an LFM pulse are within ± 0.3 GHz, ± 0.4 GHz, ± 120 ps, ± 50 mV, and ± 15 ps, respectively. Factors affecting the performance of the measurement system, such as the shape, slope, and resolution of the ACF, are discussed.

Index Terms—Instantaneous frequency measurement (IFM), linear frequency modulation (LFM), microwave photonics, optical linear filter, polarization modulation.

I. INTRODUCTION

LINEAR frequency modulation (LFM) signal is one of the most widely used pulse compression signals with a large time-bandwidth product. Due to the inherent advantages in simultaneously improving the distance and velocity accuracies of the measurement system, LFM signals have particularly extensive applications in the areas of radar, sonar, seismic survey, and secure communication. Simultaneous and instantaneous measurement of the parameters of the LFM signal such as center frequency (CF), bandwidth (BW), pulse width (PW), pulse amplitude (PA) and time of arrival (TOA) is of great importance, especially in modern electronic warfare, to analyze the intercepted RF signals from radars and communication systems. Since the frequency information is usually required for

identifying other parameters, frequency measurement should be implemented first. Although well behaved in high resolution and high flexibility, conventional electronic measurement techniques are vulnerable to electromagnetic interference (EMI). In addition, the bandwidth of the electronic measurement system is limited to about 18 GHz, due to the well-known electronic bottleneck. To solve these problems, frequency measurement based on microwave photonics is proposed [1], [2], which takes advantages of the photonic technologies, such as large bandwidth and capability to resist EMI.

In general, photonics-based frequency measurement technologies can be divided into three categories, i.e., frequency-to-space mapping, frequency-to-time mapping and frequency-to-power mapping. In the first category, microwave frequency measurement is usually implemented using an optical channelizer. The key principle of this technology is to split optical signals which are modulated by a frequency-unknown microwave signal into a number of optical channels with different center frequencies [3]–[7]. However, this kind of technology generally needs specially designed devices such as a bank of optical filters with consecutive passbands [3], optical frequency combs [4]–[7], Fabry-Perot filters with different free spectral ranges (FSRs) [4], and photodetector (PD) arrays [4]–[7]. Accordingly, schemes in this category are usually costly, bulky and very hard to design. In the second category, an inherent relationship between the time delay of the optical carrier signal and the frequency of the microwave signal is established, from which multiple frequencies can be identified simultaneously [8], [9]. The key problem associated with this method is that the resolution is limited due to the high demand for dispersive elements and optical filters. Although a resolution of a few kHz can be possibly realized, the measurement range of the system would be very small, which is usually a few MHz [10].

In the third category, the frequency of a microwave signal is instantaneously estimated by calculating an amplitude comparison function (ACF), which can be measured by monitoring and comparing two frequency-dependent optical or microwave powers. In a typical optical power monitoring based instantaneous frequency measurement (IFM) scheme, the carrier wavelengths of two carrier-suppressed double-sideband signals are set at different positions of a sinusoidal-shape filter, thus the sidebands in the two wavelength channels suffer from different power fadings. Then, the frequency of the microwave signal is estimated by monitoring and comparing the optical powers in

Manuscript received September 22, 2017; revised March 11, 2018; accepted March 14, 2018. Date of publication March 20, 2018; date of current version May 11, 2018. This work was supported in part by the National Natural Science Foundation of China under Grant 61605077, Grant 61422108, and Grant 61527820; and in part by the Fundamental Research Funds from the Central Universities. (*Corresponding authors: Xiangchuan Wang and Shilong Pan.*)

The authors are with the Key Laboratory of Radar Imaging and Microwave Photonics, Ministry of Education, Nanjing University of Aeronautics and Astronautics, Nanjing 210016, China (e-mail: bwzhang@nuaa.edu.cn; wangxch@nuaa.edu.cn; pans@ieee.org).

Color versions of one or more of the figures in this paper are available online at <http://ieeexplore.ieee.org>.

Digital Object Identifier 10.1109/JLT.2018.2817506

the two wavelength channels [11]–[13]. However, to achieve the carrier-suppressed double-sideband modulation, the Mach-Zehnder Modulator (MZM) should be biased at the minimum transmission point. Thus the bias drift of the MZM would lead to significant measurement errors. On the other hand, in the microwave power monitoring based IFM scheme, the modulators are generally biased at the quadrature points. After passing through a dispersive device, the microwave-modulated optical signals with different wavelengths [14] or different polarization states [15] experience different power fadings. By comparing the two microwave powers detected from the two optical signals, an ACF is obtained, which is monotonically increasing or decreasing with the microwave frequency. Thus, the frequency of the unknown microwave signal can be detected from the ACF. Although the two-wavelength or two-polarization-state based microwave power monitoring system behaves well in range tunability, a significant flaw of this system is that the slope of the obtained ACF is quite small, which would result in a small measurement range and a large measurement error. In order to extend the measurement range and to reduce the measurement error, complementary power fading implemented with simultaneous phase modulation (PM) and intensity modulation (IM) is utilized [16], [17]. To further simplify the system structure, a single polarization modulator (PolM) becomes an alternative [18]–[22]. In addition, other technologies such as the cascade of MZMs [23], [24] and four-wave mixing [25] are also applied for implementing frequency to microwave power mapping. As compared with the frequency-to-space mapping and frequency-to-time mapping, frequency-to-power mapping has distinct advantages in terms of simple structures, adjustable measurement range and improved measurement stability. Even if the inherent trade-off between the measurement range and resolution is still hard to eliminate, an optimal measurement range of 40 GHz and a measurement resolution of 100 MHz have been simultaneously realized [25].

The approaches discussed above are designed only for frequency measurement. Recently, we have proposed a novel approach for simultaneous measurement of multiple parameters, i.e., the frequency, amplitude, pulse width, and time of arrival of a pulsed microwave signal [26]. Although this approach has referential significance for the multi-parameter measurement of an LFM signal, the slope of the ACF varies with the microwave frequency. As a result, when acquiring the frequency of a wide-band LFM signal from the amplitude ratio, a large measurement error would arise, which further introduce measurement errors to other parameters. Thus, a linear ACF with a constant first-order derivative is required to identify the multiple parameters of the LFM signal.

In this paper, we propose, analyze and experimentally demonstrate, for the first time to the best of our knowledge, a novel photonic system that can simultaneously measure the CF, BW, PW, PA and TOA of an LFM signal. In the proposed system, a PolM together with two polarizers implements IM and PM simultaneously. The phase-modulated signal is directed into an optical linear filter to differentiate the sidebands for PM-IM conversion. Linear ACF, which is required for the multi-parameter measurement of LFM signals, is obtained by comparing the two

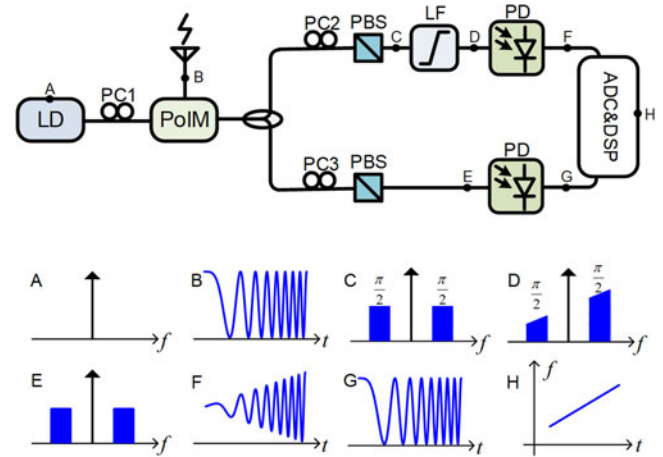


Fig. 1. Schematic of the proposed photonics-based instantaneous multi-parameter measurement system of an LFM microwave signal. LD: laser diode; PC: polarization controller; PolM: polarization modulator; PBS: polarization beam splitter; LF: linear filter; PD: photodetector; ADC: analog to digital converter; DSP: digital signal processing.

microwave powers detected from IM and the filtered PM signals. From the linear ACF, the frequency and other parameters of the LFM signal can be easily estimated. In a proof-of-concept experiment, the measurement errors for CF, BW, PW, PA and TOA of an LFM signal are within ± 0.3 GHz, ± 0.4 GHz, ± 120 ps, ± 50 mV and ± 15 ps, respectively. Because of the linear characteristic of the obtained ACF, the measurement range is only restricted to the bandwidth of the PolM and PD, which could be over 50 GHz.

II. PRINCIPLE

The schematic diagram of the proposed photonics-based instantaneous multi-parameter measurement system is shown in Fig. 1. The system consists of a laser diode (LD), a PolM, three polarization controllers (PCs), two polarization beam splitters (PBSs), an optical linear filter (LF), two PDs, two analog to digital converters (ADCs) and a signal processing module. A microwave signal with its frequency to be measured is applied to the PolM via its RF port to modulate a linearly-polarized light wave emitted from the LD. By adjusting PC1, the polarization direction of the light wave is oriented at an angle of 45° with respect to the principal axis of the PolM, to guarantee equal modulated components of the TE and TM modes. At the output of the PolM, phase-modulated TE and TM modes with the same amplitude but opposite modulation index are obtained. The modulated light wave is then divided into two branches by an optical coupler. In the lower branch, the direction of the polarizer is adjusted to have an angle of 45° with respect to the principal axis of the PolM, to obtain an intensity-modulated optical signal [18]–[22]. In the upper branch, a pure phase-modulated optical signal is achieved by aligning the direction of the polarizer to the principal axis of the PolM. The PM signal is then applied into an optical linear filter, of which the response is a linear function versus frequency. Different sidebands of the phase-modulated optical signal undergo different amplitude losses, thus a

microwave signal will be generated from the filtered optical signal at a PD, of which the amplitude is proportional to the frequency. Consequently, a linear ACF can be achieved by comparing the amplitudes of the two microwave signals.

Assume the light wave emitted from the laser diode is expressed as $E_0 \exp(j\omega_c t)$ and the microwave signal to be measured is sinusoidal, the optical field at the output of the PolM can be written as

$$\begin{bmatrix} E_x(t) \\ E_y(t) \end{bmatrix} = \frac{\sqrt{2}}{2} E_0 \exp(j\omega_c t) \begin{bmatrix} \exp(j\gamma \sin \Omega t) \\ \exp(-j\gamma \sin \Omega t + j\varphi) \end{bmatrix} \quad (1)$$

where E_0 is the amplitude of the input optical field, ω_c is the angular frequency of the optical carrier, γ is the modulation index, Ω is the angular frequency of the microwave signal, and φ is the phase difference between the TE and TM modes which can be changed by adjusting the PC after the PolM. Since a modulated light wave can be expanded to a sum of an optical carrier and many sidebands using Bessel expansion, (1) can be rewritten as

$$\begin{bmatrix} E_x(t) \\ E_y(t) \end{bmatrix} = \frac{\sqrt{2}}{2} E_0 e^{j\omega_c t} \begin{bmatrix} \dots + J_{-2}(\gamma) e^{-j2\Omega t} + J_{-1}(\gamma) e^{-j\Omega t} \\ + J_0(\gamma) \\ + J_1(\gamma) e^{j\Omega t} + J_2(\gamma) e^{j2\Omega t} + \dots \\ e^{j\varphi} \begin{bmatrix} \dots + J_{-2}(\gamma) e^{j2\Omega t} + J_{-1}(\gamma) e^{j\Omega t} \\ + J_0(\gamma) \\ + J_1(\gamma) e^{-j\Omega t} + J_2(\gamma) e^{-j2\Omega t} + \dots \end{bmatrix} \end{bmatrix} \quad (2)$$

where $J_n(*)$ represents the n th-order Bessel function of the first kind. In the lower branch, after passing through a 45° polarizer, the optical field becomes

$$E_{IM} = \frac{1}{2} E_0 \exp\left(j\omega_c t + j \cdot \frac{\varphi}{2}\right) \cdot \cos\left(\gamma \sin \Omega t - \frac{\varphi}{2}\right) \quad (3)$$

(3) is an expression of a standard intensity-modulated optical signal. When the IM signal is sent to a PD, a microwave signal will be generated with a fundamental frequency of Ω , which can be described as

$$\begin{aligned} I_1 &\approx 4k_1 \mathfrak{R}_1 |E_0|^2 \sin \frac{\varphi}{2} \cos \frac{\varphi}{2} \sin(\Omega t) \\ k_1 &= \sum_{k=0}^n (-1)^k J_k(\gamma) J_{k+1}(\gamma) \end{aligned} \quad (4)$$

where \mathfrak{R}_1 is a parameter related to the loss of the optical path and the responsibility of the PolM and PD.

In the upper branch, a 0° or 90° polarizer is implemented to select one phase-modulated component from the polarization-modulated signal which is then sent to an optical linear filter. Assume the spectral response of the filter at the frequency band of interest is $H(\omega) = K(\omega - \omega_1)$, where $H(*)$ is a linear function defined from ω_1 to ω_2 , and K is the slope. We can describe

the optical field at the output of the filter as

$$\begin{aligned} E_{PM}(t) &= \frac{\sqrt{2}}{2} E_0 e^{j\omega_c t} \begin{bmatrix} \dots + K(\omega_c - 2\Omega - \omega_1) J_{-2}(\gamma) e^{-j2\Omega t} \\ + K(\omega_c - \Omega - \omega_1) J_{-1}(\gamma) e^{-j\Omega t} \\ + K J_0(\gamma) (\omega_c - \omega_1) \\ + K(\omega_c + \Omega - \omega_1) J_1(\gamma) e^{j\Omega t} \\ + K(\omega_c + 2\Omega - \omega_1) J_2(\gamma) e^{j2\Omega t} + \dots \end{bmatrix} \end{aligned} \quad (5)$$

As shown in (5), after passing through the optical linear filter, differentiation between the sidebands of the PM signal is realized. The sidebands-differentiated PM signal is then sent to a PD for square-law detection. The fundamental frequency term of the photocurrent can be written as

$$\begin{aligned} I_2 &\approx 2k_2 \mathfrak{R}_2 |E_0|^2 K^2 (\omega_c - \omega_1) \Omega \cos(\Omega t) \\ k_2 &= \sum_{k=0}^n (2k+1) J_k(\gamma) J_{k+1}(\gamma) \end{aligned} \quad (6)$$

The amplitude ratio of the two photocurrents in (4) and (6) is given by

$$\begin{aligned} \text{ACF}(f) &= \frac{\text{amp}(I_2)}{\text{amp}(I_1)} = \frac{k_2}{k_1} \frac{\mathfrak{R}_2}{2\mathfrak{R}_1 \sin \frac{\varphi}{2} \cos \frac{\varphi}{2}} K^2 (\omega_c - \omega_1) \Omega \\ \frac{k_2}{k_1} &= \frac{[\sum_{k=0}^n (2k+1) J_k(\gamma) J_{k+1}(\gamma)]}{[\sum_{k=0}^n (-1)^k J_k(\gamma) J_{k+1}(\gamma)]} \end{aligned} \quad (7)$$

where $f = \Omega/2\pi$. \mathfrak{R}_1 and \mathfrak{R}_2 can be made identical by adjusting the losses of the optical paths via optical attenuators. By adjusting the PC after the PolM, φ can be fixed to $\pi/2$. As a result, the ACF is directly proportional to the frequency of the unknown microwave signal and is independent of the input optical power.

When the signal to be measured is a small signal, i.e., $J_0(\gamma) \approx 1$, $J_1(\gamma) \approx \gamma/2$ and $J_n(\gamma) \approx 0$ for $n \geq 2$, only the first-order sidebands need to be considered. On this condition, (4), (6) and (7) degenerate into the following expressions

$$I_1' \approx 4\mathfrak{R}_1 |E_0|^2 \frac{\gamma}{2} \sin \frac{\varphi}{2} \cos \frac{\varphi}{2} \sin(\Omega t) \quad (8)$$

$$I_2' \approx 2\mathfrak{R}_2 |E_0|^2 K^2 \frac{\gamma}{2} (\omega_c - \omega_1) \Omega \cos(\Omega t) \quad (9)$$

$$\text{ACF}'(f) = \frac{\text{amp}(I_2)}{\text{amp}(I_1)} = \frac{\mathfrak{R}_2}{2\mathfrak{R}_1 \sin \frac{\varphi}{2} \cos \frac{\varphi}{2}} K^2 (\omega_c - \omega_1) \Omega \quad (10)$$

Based on the linear ACF in (10), the frequency of the unknown microwave signal can be directly estimated,

$$f = \kappa \times \text{ACF} \quad (11)$$

where $\kappa = 1/[2\pi K^2(\omega_c - \omega_1)]$, a parameter that is independent of the amplitude of the input microwave signal. Different from other ACF-based IFM systems, the slope of the ACF in our system is constant, which guarantees a maximized measurement range on the condition of a given measurement error. Besides,

thanks to the linear characteristics of the ACF, only a reference microwave signal with a fixed frequency is sufficient for obtaining an accurate κ before the measurement, which greatly simplifies the calibration process.

The system is also capable of measuring the multiple parameters of a pulsed signal, e.g., an LFM microwave signal, due to the linear characteristics of the ACF. Mathematically, a pulsed LFM microwave signal to be measured is expressed as

$$s_{\text{LFM}}(t) = V_e R(t) \sin \left[\omega_0(t - t_{\text{TOA}}) + \frac{1}{2}k(t - t_{\text{TOA}})^2 \right] \quad (12)$$

where V_e is the amplitude, $R(t)$ is the normalized pulse profile which has nonzero value from t_{TOA} to $t_{\text{TOA}} + t_{\text{PW}}$ in a single pulse cycle, t_{TOA} is the arrival time, t_{PW} is the pulse width, and k is the chirp rate of the LFM signal. Then, the modulation index γ can be denoted as

$$\gamma(t) = \pi \frac{V_e}{V_\pi} R(t) \quad (13)$$

and (8), (9) and (10) can be rewritten as

$$I_{\text{LFM-IM}} \approx 4\Re_1 |E_0|^2 \frac{\gamma(t)}{2} \sin \frac{\varphi}{2} \cos \frac{\varphi}{2} \cdot \sin \left(\omega_0(t - t_{\text{TOA}}) + \frac{1}{2}k(t - t_{\text{TOA}})^2 \right) \quad (14)$$

$$I_{\text{LFM-PM}} \approx 2\Re_2 |E_0|^2 K^2 \frac{\gamma(t)}{2} (\omega_c - \omega_1) (\omega_0 + k(t - t_{\text{TOA}})) \cdot \cos \left(\omega_0(t - t_{\text{TOA}}) + \frac{1}{2}k(t - t_{\text{TOA}})^2 \right) \quad (15)$$

$$\begin{aligned} \text{ACF}_{\text{LFM}}(t) &= \frac{\text{amp}(I_{\text{LFM-PM}})}{\text{amp}(I_{\text{LFM-IM}})} \\ &= \frac{\Re_2}{2\Re_1 \sin \frac{\varphi}{2} \cos \frac{\varphi}{2}} K^2 (\omega_c - \omega_1) [\omega_0 + k(t - t_{\text{TOA}})] \\ &= \kappa \cdot [\omega_0 + k(t - t_{\text{TOA}})] \end{aligned} \quad (16)$$

From (16), the ACF of the LFM signal as a function of time is independent of $V_e R(t)$, i.e., the amplitude of the signal, so the instantaneous frequency of the LFM signal can be accurately identified by monitoring the ACF, which leads to the measurement of CF, BW.

From (14), we have

$$V_e R(t) = \frac{\text{amp}(I_{\text{LFM-IM}}) V_\pi}{\pi \Re_1 |E_0|^2 \sin \varphi} \quad (17)$$

In practice, the amplitude of $I_{\text{LFM-IM}}$ can be obtained by a microwave detector together with a low-speed ADC, and $V_\pi / (\pi \Re_1 |E_0|^2 \sin \varphi)$ is achievable in the calibration process, so $V_e R(t)$ can be estimated. Since the PW, PA and TOA are all included in $V_e R(t)$, they can also be identified.

III. EXPERIMENT RESULTS AND DISCUSSION

A proof-of-concept experiment is carried out based on the configuration shown in Fig. 1. A light wave at 1550.5 nm is emitted from a tunable laser source (Agilent N7714A) with an output power of 16 dBm and a linewidth of 12 kHz. The light

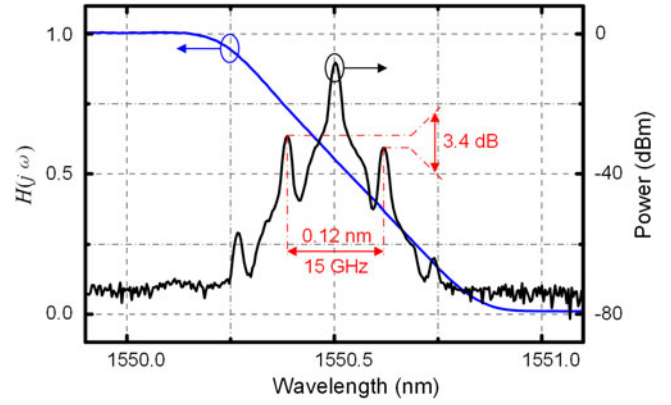


Fig. 2. Spectral response of the filter and the optical spectrum of the sideband-differentiated PM signal carrying a 15-GHz microwave signal.

wave is modulated by a microwave signal generated by a vector network analyzer (VNA, R&S) or an AWG (Keysight M8195A) at a 40-Gb/s PolM (Versawave Technologies). The polarization-modulated signal is then split into two branches by an optical coupler. In the upper branch, the optical signal along one principal polarization direction of the PolM is selected by a polarizer implemented by a PC and a PBS, so a phase-modulated signal is obtained, which is sent to an optical linear filter implemented by a programmable optical processor (Finisar waveshaper 4000s). The linear region of the filter is from 1550.1 to 1550.9 nm, as shown in Fig. 2. Located at the center of the linear region, the selected phase-modulated signal is first-order differentiated and sent to a 40-GHz PD (u2t XPDV2120R). In the lower branch, an IM signal is generated from the polarization-modulated signal by a 45° polarizer and directly sent to a PD. The electrical signals converted by the PDs are measured by the VNA or a real-time oscilloscope (Agilent DSO-X 92504A). An optical spectrum analyzer (YOKOGAWA AQ6370C) is also used to monitor the optical signals in the system.

A. Linear ACF for Microwave Measurement

To investigate the performance of the proposed measurement system, firstly we apply a single-frequency microwave signal to the RF port of the PolM. Fig. 2 shows the spectral response of the filter and the spectrum of the filtered optical signal carrying a 15-GHz microwave signal. The linear region of the designed optical filter is 100 GHz, and the center wavelength of the optical carrier is set at the center of the filter. Thanks to the linearly filtering, the two sidebands of the PM signal have a power imbalance of 3.4 dB, so a microwave signal can be generated if the filtered optical signal is sent to a PD. Then, the frequency of the input microwave signal, which is generated from the VNA, is swept from 0 to 40 GHz. The power of the microwave signal is set as 0 dBm, which can be regarded as a small signal to the measurement system. Fig. 3 shows the two frequency-dependent microwave power penalty functions measured by the VNA. The amplitude ripples existing in both curves can be eliminated by comparison, which produces a linear ACF with a constant slope over the entire frequency range from 0 to 40 GHz, as shown

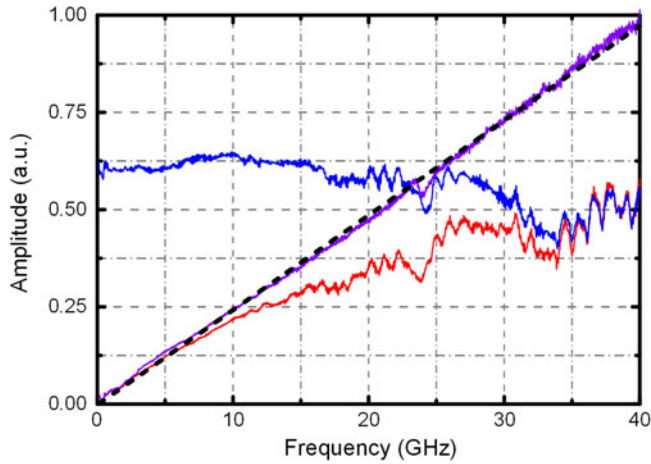


Fig. 3. Amplitudes of the photocurrents generated from the IM signal (blue line) and the first-order differentiated PM signal (red line), and the calculated ACF.

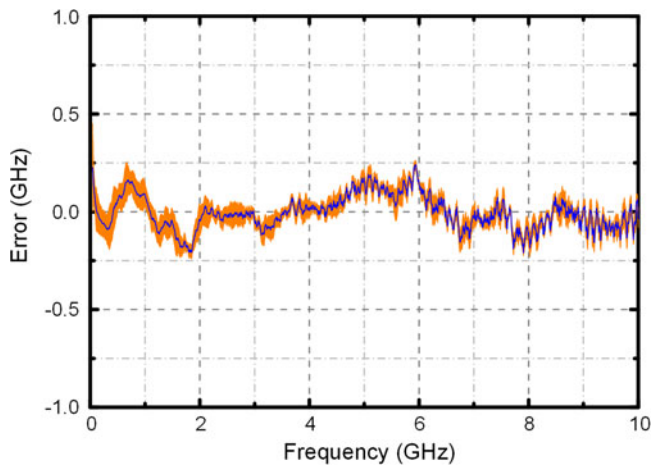


Fig. 4. Frequency measurement error versus input microwave frequency for CW signals. Orange area: the distribution of the frequency errors among ten measurements; blue line: the mean error.

in Fig. 3. With this linear ACF, the microwave frequency can be easily estimated by measuring the microwave powers and calculating the power ratio.

By fitting the experimental results shown in Fig. 3, the measurement error of CW microwave signal in our system can be calculated. Fig. 4 shows the frequency measurement error versus input microwave frequency for ten measurements. As can be seen, a frequency measurement error within ± 0.25 GHz is obtained when the input frequency varies from 0 to 10 GHz. Because the slope of our ACF is almost the same, the measurement error among all frequency ranges keeps at a relatively low value. At the same time, thanks to the waveshaper, which is a programmable filter, the slope and the frequency range of the optical linear filter can be adjusted arbitrarily. Thus a range adjustable measurement system can be obtained. Similar to previous works, the measurement accuracy of the system is also influenced by the imperfect performance of the electrical devices used in this experiment. Another important factor is the polarization jitter. Due to the use of the PolM, simultaneous

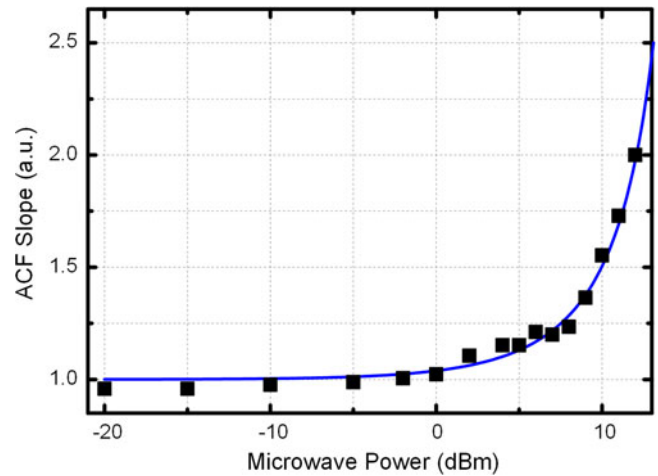


Fig. 5. The slope of ACF versus the microwave power.

phase-modulated and intensity-modulated signals are generated by selecting proper polarization components using a PC and a PBS, so the polarization jitter would inevitably affect the generation of pure phase-modulated and intensity-modulated signals. To further improve the measurement accuracy of the system, accurate polarization control needs to be incorporated.

It is noteworthy that (11) is obtained on the condition of small signal approximation. But in practice, the microwave power is not always small. When the power of the input microwave signal is large, the small signal approximation is not applicable and contributions from the high-order harmonics need to be considered. In this case, we can measure the ACF using (7), in which all orders of the Bessel functions are included.

Based on (7), the slope of the ACF can be measured or calculated as a function of the microwave power. Fig. 5 compares the actual and simulated slopes of the ACF versus the microwave power. Among a range from -20 to 0 dBm, the slope of the ACF keeps almost unchanged, while for microwave powers over 0 dBm, it is monotonically increasing, which indicates that an automatic gain controller should be used to control the input microwave power to be smaller than 0 dBm to ensure an accurate measurement.

Another factor which has an important impact on the performance of the system is the linearity of the optical linear filter. In practice, the linearity of the optical filter is not usually so perfect, and the phase response of the optical filter is not so flat either. As a result, we can observe some small notches in the calculated ACF in Fig. 3. This problem might be solved by carefully design the frequency response of the programmable optical processor via the feedback provided by an ultra-high resolution optical vector analyzer [27].

B. Multi-parameter Measurement of LFM signals

With the linear ACF, the instantaneous frequency of an LFM signal can be measured. Fig. 6(a) shows the temporal profiles of the LFM signals from the IM and PM branches. Due to the amplitude variation of the original LFM signal from the AWG and the uneven frequency responses of the PolM and the PD,

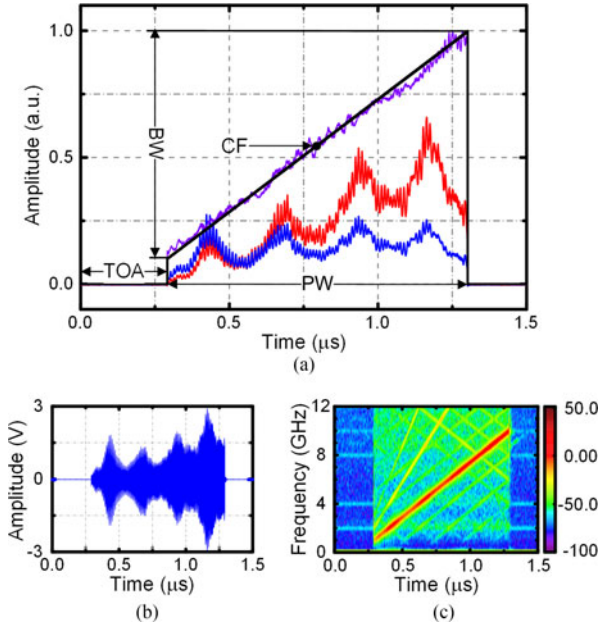


Fig. 6. (a) The temporal profiles of the LFM signals from the IM (blue line) and PM (red line) branches, the calculated instantaneous frequency of the LFM signal (purple line). (b) The waveform of the LFM signal from the IM branch. (c) The instantaneous frequency obtained by short-time Fourier transform analysis.

the amplitudes of the two profiles are with large ripples. By calculating the amplitude ratio, however, amplitude unevenness is eliminated and a linear frequency-time curve is obtained, as shown as the purple line in Fig. 6(a). The frequency range is from 1 to 10 GHz, the center frequency is 5.5 GHz, the pulse width is 1 μ s, and the TOA is 0.291 μ s. In addition, the pulse amplitude can be also obtained from the temporal profile of the signal from the IM branch, of which the frequency response is measured by the VNA. To validate the measurement, we record the waveform of the LFM signal from the IM branch and calculate the instantaneous frequency using short time Fourier transform (STFT), with the results shown in Figs. 6(b) and (c). As can be seen, the measured curve is in line with the one calculated using STFT, which confirms the feasibility of the proposed method for accurate measurement of the multiple parameters of LFM signals.

Fig. 7 shows the measured CF, BW, PW, PA and TOA using the proposed method versus the actual data. When the CF of the modulated LFM signal varies from 1.5 to 9.5 GHz, the measurement error is within ± 0.3 GHz. The error of the BW measurement is ± 0.4 GHz within a frequency bandwidth range of 1–10 GHz. For the measurement of PA, we obtain an error of ± 50 mV within a range of 0–1 V. The measurement errors of the PW and TOA are ± 120 ps and ± 15 ps respectively. It should be noted that the TOA in Fig. 5(e) has already excluded the fixed delay of 20.8 ns, which is mainly resulted from the link length of the measurement system.

IV. DISCUSSION

Dynamic range is one key performance indicator of the multi-parameter measurement system. In order to obtain the dynamic

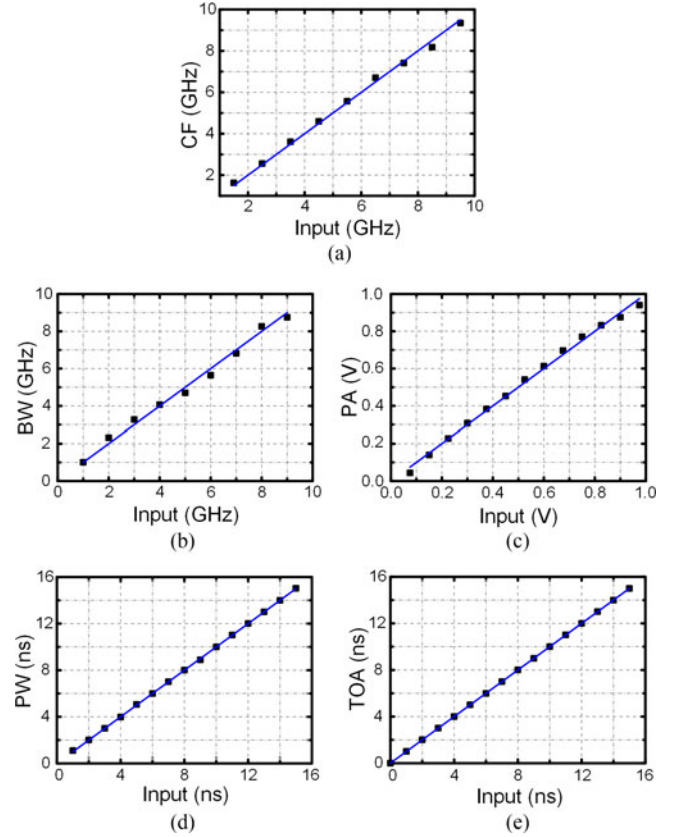


Fig. 7. The measured (a) CF, (b) BW, (c) PA, (d) PW and (e) TOA versus the actual ones.

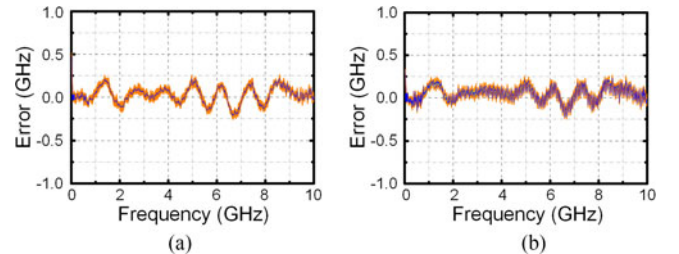


Fig. 8. Frequency errors of ten measurements when the input microwave powers are (a) 13 dBm and (b) -18 dBm, respectively. Orange area: the distribution of the frequency errors among ten measurements; blue line: the mean error.

range of the proposed system, the power of the input microwave signal is changed and the corresponding measurement errors are measured. Fig. 8(a) shows the measurement error when the input microwave power is 13 dBm, while Fig. 8(b) shows the case when the input microwave power is -18 dBm. As can be seen, the minimum microwave power required to achieve a measurement error of ± 250 MHz is lower than -18 dBm.

As has been discussed in the experiment part, the polarization states before and after the PoIM are directly related to the frequency measurement error. Another important factor which has a great influence on the frequency measurement error is the slope of the optical linear filter. A smaller slope of the filter corresponds to a larger measurement range but a smaller signal after the PD and therefore a larger frequency measurement error, and vice versa. Fig. 9 shows the relationship between the

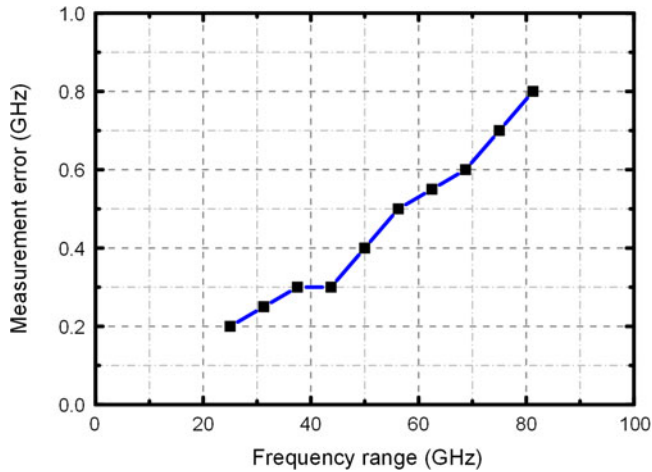


Fig. 9. Measurement error versus frequency range of the input microwave signal.

measurement error and the linear frequency range of the waveshaper. As can be seen, there is trade-off between frequency measurement range and frequency measurement resolution. According to (17), the PA, PW and TOA are independent of frequency. Thus the changing of the frequency range has no influence on the measurement results of PA, PW and TOA.

In our work, the measurement errors for CF, BW, PW, PA and TOA of an LFM pulse are within ± 0.3 GHz, ± 0.4 GHz, ± 120 ps, ± 50 mV and ± 15 ps, respectively. For a comparison, the CF, PW and TOA measurement resolutions of a typical electronic IFM receiver (Wide Band Systems Inc.) are about ± 1 MHz, ± 25 ns and ± 25 ns [28], and the measurement errors for the PA, PW and TOA of a photonic IFM receiver [26] are ± 50 mV, ± 1 ns and ± 0.16 ns, respectively. It should be noted that the IFM systems in [26] and [28] are mainly used to measure inter-pulse parameters while the proposed approach can achieve intra-pulse frequencies. Since the frequency resolution of the proposed approach is relatively poor for practical applications, further improvements need to be carried out, such as accurate control of the polarization, precious design of the optical linear filter and increase of the effective number of bits (ENOBs) of the ADC.

V. CONCLUSION

We have proposed and experimentally demonstrated a photonic approach to measure the CF, BW, PW, PA and TOA of an LFM signal simultaneously. This technology is implemented utilizing a linear ACF which is implemented based on frequency to microwave power mapping. The key element of this system is a PolM, which can be used to simultaneously realize PM and IM by simply adjusting the PCs between the PolM and the PBSs. Thanks to the linearity of the optical filter, the first-order sidebands of the PM signal are differentiated. Thus a linear ACF is obtained by calculating the power ratio of the photocurrents generated from the PM signal and IM signal. Based on the calculated ACF, the multi-parameter of an LFM signal are estimated. In the experiment, multi-parameter measurement of an LFM microwave signal is completed with a CF accuracy

of ± 0.3 GHz, a BW accuracy of ± 0.4 GHz, a PA accuracy of ± 50 mV, a PW accuracy of ± 120 ps, and a TOA accuracy of ± 15 ps. The proposed system is multi-functional and compact, which can find applications in modern electromagnetic counter-measure systems.

REFERENCES

- [1] S. L. Pan and J. P. Yao, "Photonics-based broadband microwave measurement," *J. Lightw. Technol.*, vol. 35, no. 16, pp. 3498–3513, Aug. 2017.
- [2] X. H. Zou, B. Lu, W. Pan, L. S. Yan, A. Stohr, and J. P. Yao, "Photonics for microwave measurements," *Laser Photon. Rev.*, vol. 10, no. 5, pp. 711–734, Sep. 2016.
- [3] D. B. Hunter and R. A. Minasian, "Microwave optical filters using in-fiber Bragg grating arrays," *IEEE Microw. Guided Wave Lett.*, vol. 6, no. 2, pp. 103–105, Feb. 1996.
- [4] X. J. Xie *et al.*, "Broadband photonic radio-frequency channelization based on a 39-GHz optical frequency comb," *IEEE Photon. Technol. Lett.*, vol. 24, no. 8, pp. 661–663, Apr. 2012.
- [5] X. H. Zou, W. Pan, B. Luo, and L. S. Yan, "Photonic approach for multiple-frequency-component measurement using spectrally sliced incoherent source," *Opt. Lett.*, vol. 35, no. 3, pp. 438–440, Feb. 2010.
- [6] W. Y. Xu, D. Zhu, and S. L. Pan, "Coherent photonic RF channelization based on dual coherent optical frequency combs and stimulated Brillouin scattering," *Opt. Eng.*, vol. 55, no. 4, Apr. 2016, Art. no. 046106.
- [7] A. O. J. Wiberg *et al.*, "Coherent filterless wideband microwave/millimeter-wave channelizer based on broadband parametric mixers," *J. Lightw. Technol.*, vol. 32, no. 20, pp. 3609–3617, Oct. 2014.
- [8] L. V. T. Nguyen, "Microwave photonic technique for frequency measurement of simultaneous signals," *IEEE Photon. Technol. Lett.*, vol. 21, no. 10, pp. 642–644, May 2009.
- [9] T. A. Nguyen, E. H. W. Chan, and R. A. Minasian, "Instantaneous high-resolution multiple-frequency measurement system based on frequency-to-time mapping technique," *Opt. Lett.*, vol. 39, no. 8, pp. 2419–2422, Apr. 2014.
- [10] H. G. de Chatellus, L. R. Cortes, and J. Azana, "Optical real-time Fourier transformation with kilohertz resolutions," *Optica*, vol. 3, no. 1, pp. 1–8, Jan. 2016.
- [11] H. Chi, X. H. Zou, and J. P. Yao, "An approach to the measurement of microwave frequency based on optical power monitoring," *IEEE Photon. Technol. Lett.*, vol. 20, no. 14, pp. 1249–1251, Jul. 2008.
- [12] Z. Li, C. Wang, M. Li, H. Chi, X. M. Zhang, and J. P. Yao, "Instantaneous microwave frequency measurement using a special fiber Bragg grating," *IEEE Microw. Wireless Compon. Lett.*, vol. 21, no. 1, pp. 52–54, Jan. 2011.
- [13] X. H. Zou, H. Chi, and J. P. Yao, "Microwave frequency measurement based on optical power monitoring using a complementary optical filter pair," *IEEE Trans. Microw. Theory Techn.*, vol. 57, no. 2, pp. 505–511, Feb. 2009.
- [14] X. H. Zou and J. P. Yao, "An optical approach to microwave frequency measurement with adjustable measurement range and resolution," *IEEE Photon. Technol. Lett.*, vol. 20, no. 23, pp. 1989–1991, Dec. 2008.
- [15] Z. Y. Tu, A. J. Wen, Y. S. Gao, W. Chen, Z. X. Peng, and M. Chen, "A photonic technique for instantaneous microwave frequency measurement utilizing a phase modulator," *IEEE Photon. Technol. Lett.*, vol. 28, no. 24, pp. 2795–2798, Dec. 2016.
- [16] N. N. Shi, Y. Y. Gu, J. J. Hu, Z. J. Kang, X. Y. Han, and M. S. Zhao, "Photonic approach to broadband instantaneous microwave frequency measurement with improved accuracy," *Opt. Commun.*, vol. 328, pp. 87–90, Oct. 2014.
- [17] J. Q. Zhou, S. N. Fu, S. Aditya, P. P. Shum, and C. L. Lin, "Instantaneous microwave frequency measurement using photonic technique," *IEEE Photon. Technol. Lett.*, vol. 21, no. 15, pp. 1069–1071, Aug. 2009.
- [18] J. Li *et al.*, "Performance analysis on an instantaneous microwave frequency measurement with tunable range and resolution based on a single laser source," *Opt. Laser Technol.*, vol. 63, pp. 54–61, Nov. 2014.
- [19] Y. Q. Li *et al.*, "Instantaneous microwave frequency measurement with improved resolution," *Opt. Commun.*, vol. 354, pp. 140–147, Nov. 2015.
- [20] X. H. Zou, S. L. Pan, and J. P. Yao, "Instantaneous microwave frequency measurement with improved measurement range and resolution based on simultaneous phase modulation and intensity modulation," *J. Lightw. Technol.*, vol. 27, no. 23, pp. 5314–5320, Dec. 2009.

- [21] Y. Q. Li, L. Pei, J. Li, Y. Q. Wang, and J. Yuan, "Theory study on a range-extended and resolution-improved microwave frequency measurement," *J. Mod. Opt.*, vol. 63, no. 7, pp. 613–620, Sep. 2015.
- [22] S. L. Pan and J. P. Yao, "Instantaneous microwave frequency measurement using a photonic microwave filter pair," *IEEE Photon. Technol. Lett.*, vol. 22, no. 19, pp. 1437–1439, Oct. 2010.
- [23] H. Emami, N. Sarkhosh, L. A. Bui, and A. Mitchell, "Amplitude independent RF instantaneous frequency measurement system using photonic Hilbert transform," *Opt. Express*, vol. 16, no. 18, pp. 13707–13712, Sep. 2008.
- [24] N. Sarkhosh, H. Emami, L. Bui, and A. Mitchell, "Reduced cost photonic instantaneous frequency measurement system," *IEEE Photon. Technol. Lett.*, vol. 20, no. 18, pp. 1521–1523, Sep. 2008.
- [25] H. Emami and M. Ashourian, "Improved dynamic range microwave photonic instantaneous frequency measurement based on four-wave mixing," *IEEE Trans. Microw. Theory Techn.*, vol. 62, no. 10, pp. 2462–2470, Oct. 2014.
- [26] S. L. Pan, J. B. Fu, and J. P. Yao, "Photonic approach to the simultaneous measurement of the frequency, amplitude, pulse width, and time of arrival of a microwave signal," *Opt. Lett.*, vol. 37, no. 1, pp. 7–9, Jan. 2012.
- [27] S. L. Pan and M. Xue, "Ultrahigh-resolution optical vector analysis based on optical single-sideband modulation," *J. Lightw. Technol.*, vol. 35, no. 4, pp. 836–845, Feb. 2017.
- [28] "Digital IFM system receivers," Wide Band Systems, Rockaway, NJ, USA, 2017. [Online]. Available: http://widebandsystems.com/wp-content/uploads/2017/09/Digital_IFM_System_Receivers.pdf

Bowen Zhang received the B.S. degree in electronics engineering from Tsinghua University, Beijing, China, in 2016. He is currently working toward the Ph.D. degree at the Key Laboratory of Radar Imaging and Microwave Photonics, Ministry of Education, Nanjing University of Aeronautics and Astronautics, Nanjing, China.

His research interests include photonic microwave measurement and photonic technologies for signal processing.

Xiangchuan Wang received the B.Eng. degree in automation and the Ph.D. degree in microelectronics and solid-state electronics from Nanjing University, Nanjing, China, in 2009 and 2015, respectively.

He is currently a Lecturer with the Key Laboratory of Radar Imaging and Microwave Photonics, Ministry of Education, Nanjing University of Aeronautics and Astronautics, Nanjing, China. His current research interests are in microwave photonic measurement and optical fiber sensing technologies.

Shilong Pan (S'06–M'09–SM'13) received the B.S. and Ph.D. degrees in electronics engineering from Tsinghua University, Beijing, China, in 2004 and 2008, respectively.

From 2008 to 2010, he was a "Vision 2010" Postdoctoral Research Fellow with the Microwave Photonics Research Laboratory, University of Ottawa, Ottawa, ON, Canada. In 2010, he joined the College of Electronic and Information Engineering, Nanjing University of Aeronautics and Astronautics, Nanjing, China, where he is currently a Full Professor and the Executive Director with the Key Laboratory of Radar Imaging and Microwave Photonics, Ministry of Education. His research focuses on microwave photonics, which includes optical generation and processing of microwave signals, analog photonic links, photonic microwave measurement, and integrated microwave photonics. He has authored or coauthored more than 340 research papers, including more than 180 papers in peer-reviewed journals and 160 papers in conference proceedings. He is currently a Topical Editor for the *Chinese Optics Letters*. He was the recipient of an OSA Outstanding Reviewer Award in 2015 and a Top Reviewer for the JOURNAL OF LIGHTWAVE TECHNOLOGY in 2016. He is a Chair of numerous international conferences and workshops, including the TPC Chair of the International Conference on Optical Communications and Networks in 2015, the TPC Co-Chair for the IEEE International Topical Meeting on Microwave Photonics in 2017, the TPC Chair of the high-speed and broadband wireless technologies subcommittee of the IEEE Radio Wireless Symposium in 2013, 2014, and 2016, the TPC Chair of the Optical fiber sensors and microwave photonics subcommittee of the OptoElectronics and Communication Conference in 2015, and a Chair of the microwave photonics for broadband measurement workshop of International Microwave Symposium in 2015.